Photoinduced Ligand Redistribution Chemistry of Quadruply Bonded $Mo_2Cl_2(6\text{-mhp})_2(PR_3)_2$ Complexes

Ann M. Macintosh and Daniel G. Nocera*

Department of Chemistry, Michigan State University, East Lansing, Michigan 48824

Received March 7, 1996[⊗]

The quadruply bonded metal−metal complexes *cis*-$Mo_2Cl_2(6\text{-mhp})_2(PR_3)_2$ (R_3 = Et_3, Me_3, Me_2Ph, $MePh_2$; 6-mhp = 2-hydroxy-6-methylpyridinato) photoreact when their solutions are irradiated with visible and near-UV light. The primary photoprocess leads to the ligand redistribution products $Mo_2Cl_3(6\text{-mhp})(PR_3)_3$ and $Mo_2Cl(6\text{-mhp})_3(PR_3)$. In THF at room temperature, these photoproducts are stable and over time they back-react completely to the starting material. Photolysis of *cis*-$Mo_2Cl_2(6\text{-mhp})_2(PR_3)_2$ in DMF results in the same products; however, $Mo_2Cl_3(6\text{-mhp})(PR_3)_3$ rapidly decomposes, leaving $Mo_2Cl(6\text{-mhp})_3(PR_3)$ as the only isolable photoproduct. Conversely, when the reaction is carried out in benzene, $Mo_2Cl(6\text{-mhp})_3(PR_3)$ undergoes a slow secondary photoreaction and $Mo_2Cl_3(6\text{-mhp})(PR_3)_3$ is the photoproduct that is isolated. At a given wavelength, the photolysis quantum yield (Φ_p) increases along the solvent series C_6H_6 < THF < DMF ($\Phi_p{}^{405}$ = 0.00042, 0.00064, and 0.00097, respectively, for *cis*-$Mo_2Cl_2(6\text{-mhp})_2(PMe_2Ph)_2$). For a given solvent, Φ_p increases with decreasing excitation wavelength ($\Phi_p{}^{546} = 0.00012$, $\Phi_p{}^{436} = 0.00035$, $\Phi_p{}^{405} = 0.00042$, $\Phi_p{}^{366} = 0.0022$, and $\Phi_p{}^{313} = 0.0079$ in C_6H_6). This wavelength dependence of the photoreaction quantum yield in conjunction with the excitation spectrum establishes that the photoreaction does not originate from the lowest energy $\delta\delta^*$ excited state, which possesses a long lifetime and an appreciable emission quantum yield in C_6H_6, CH_2Cl_2, THF, and DMF. The photochemistry is instead derived from higher energy excited states with the maximum photoreactivity observed for excitation wavelengths coinciding with absorption features previously assigned to ligand-to-metal charge transfer transitions.

Introduction

The electronic excited states of quadruply bonded metal−metal complexes, $M\overset{4}{-}M$, offer the opportunity to photochemically promote multielectron transformations. Excitation of the coordinatively unsaturated, electron-rich d^4-d^4 core produces metal-localized excited states with significant zwitterionic character ($^+M-M:^-$).[1] We have shown that the reduced metal of this zwitterionic center is efficiently trapped by substrates in a discrete two-electron step to yield d^3-d^3 complexes.[2] This multielectron photochemistry is facilitated by an increase in the coordination number of the bimetallic center upon its two-electron oxidation. Depending on the coordination environment of the $M\overset{4}{-}M$ parent complex, different geometries are enforced in the photoproduct, as shown in Scheme 1. With the geometry of the transverse plane rigidly defined by the bridging $\overline{\mathrm{P\,P}}$ ligands in D_{2h} complexes, the two-electron photooxidative addition of substrate is promoted by two terminal halide ligands folding into edge-bridging positions to yield edge-sharing bioctahedral photoproducts (ESBOs). For example, *trans*-$M_2X_4(\overline{\mathrm{P\,P}})_2$ ($\overline{\mathrm{P\,P}}$ = bidentate phosphine, M = Mo(II) or W(II), X = halide) complexes photooxidatively add a variety of substrates (YZ) to yield $M_2X_4YZ(\overline{\mathrm{P\,P}})_2$ ESBOs.[3] Conversely, the absence of bridging ligands in $M_2X_4P_4$ (D_{2d}) complexes (X = halide, P = terminal phosphine) allows three terminal halides to move into bridging positions about the photooxidized bimetallic core to afford face-sharing bioctahedral products (FSBOs).[4] We wondered whether different photoproduct coordination geometries might be obtained when the $M\overset{4}{-}M$ complex was not of D_{2d} or D_{2h} parentage. Specifically, will the photooxidation of $M\overset{4}{-}M$ complexes with two bridging bidentate ligands in a cis arrangement result in W-frame (or cradle) products? In the W-frame structure type, two metals are supported by two bidentate ligands, which span the metal centers in a cis,cis conformation, and four additional ligands, two of which occupy bridging positions.[5−7] From the perspective of elaborating $M\overset{4}{-}M$ photocatalysis, W-frame complexes are interesting be-

Scheme 1

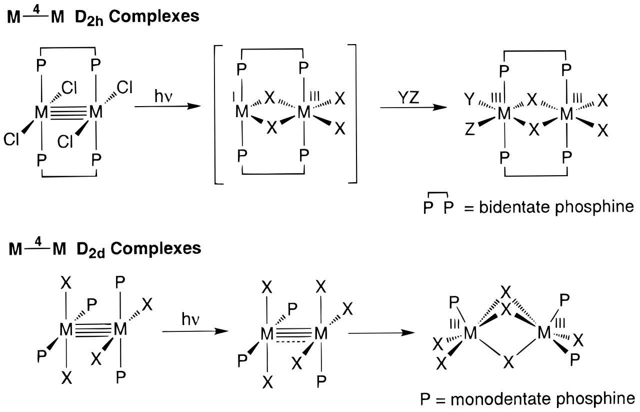

[⊗] Abstract published in *Advance ACS Abstracts,* October 15, 1996.

(1) Engebretson, D. S.; Zaleski, J. M.; Leori, G. E.; Nocera, D. G. *Science* **1994**, *265*, 759−62.

(2) (a) Nocera, D. G. *Acc. Chem. Res.* **1995**, *28*, 209−17. (b) Nocera, D. G. *J. Cluster Sci.* **1994**, *5*, 185−209.

(3) (a) Hsu, T.-L. C.; Helvoigt, S. A.; Partigianoni, C. M.; Turró, C.; Nocera, D. G. *Inorg. Chem.* **1995**, *34*, 6186−90. (b) Partigianoni, C. M.; Nocera, D. G. *Inorg. Chem.* **1990**, *29*, 2033−4.

(4) Hsu, T.-L. C.; Engebretson, D. S.; Helvoigt, S. A.; Nocera, D. G. *Inorg. Chim. Acta* **1995**, *240*, 551−7.

(5) Cotton, F. A.; Dunbar, K. R.; Verbruggen, M. G. *J. Am. Chem. Soc.* **1987**, *109*, 5498−506.

(6) Wu, J.; Fanwick, P. E.; Kubiak, C. P. *J. Am. Chem. Soc.* **1989**, *111*, 7812−23.

(7) Shih, K.; Fanwick, P. E.; Walton, R. A. *Inorg. Chem.* **1992**, *31*, 3663−8.

S0020-1669(96)00252-2 CCC: $12.00

cause they offer a rational framework in which to regenerate a $M\overset{4}{-}M$ parent complex by reductive elimination,[6] which is a reaction that is facilitated by the proximity of the two bridging ligands in the W-frame structure.

The quadruply bonded $Mo_2Cl_2(6\text{-mhp})_2(PR_3)_2$ (mhp = 2-hydroxy-6-methylpyridinato; PR_3 = phosphine) complexes are photoactive $M\overset{4}{-}M$ complexes possessing bidentate ligands in a cis conformation. The compounds have been prepared with PR_3 = PEt_3, PMe_2Ph, and $PMePh_2$,[8,9] and the crystal structure of the PEt_3 complex reveals that the mhp ligands assume a cis conformation with the methyl groups of the pyridinato ligand in a head-to-tail arrangement. Low-temperature spectroscopy is consistent with a $\delta \rightarrow \delta^*$ assignment for the lowest-energy absorption band,[8] arising from a δ-HOMO and a δ^*-LUMO of a $\sigma^2\pi^4\delta^2$ ground state electronic configuration.[10] The presence of a long-lived $\delta\delta^*$ excited state (τ_0 = 34 ns for the PEt_3 complex[8]) in principle permits the excited state oxidation chemistry for this series of complexes to be elaborated. However, as we now report for this series of complexes, which has been extended to include the compound with PR_3 = PMe_3, well-defined photoredox chemistry is obscured by facile photoinduced redistribution of the mhp ligands.

Experimental Section

General Procedures. All manipulations were carried out under an atmosphere of dry argon using standard Schlenk-line techniques. Solvents were dried, freshly distilled, and deoxygenated prior to use according to standard methods. Trimethylsilyl chloride and 2-hydroxy-6-methylpyridine (Hmhp) were purchased from Aldrich Chemical Co. and were used without further purification. Tertiary phosphines were obtained from Strem Chemicals Inc. and stored under argon.

Syntheses. The complexes *cis*-$Mo_2Cl_2(6\text{-mhp})_2(PMe_2Ph)_2$, *cis*-$Mo_2Cl_2(6\text{-mhp})_2(PMePh_2)_2$, *cis*-$Mo_2Cl_2(6\text{-mhp})_2(PEt_3)_2$, and $Mo_2Cl_3(6\text{-mhp})(PMe_2Ph)_3$ were prepared by published procedures[9] as was $Mo_2(mhp)_4$.[11] The complex *cis*-$Mo_2Cl_2(6\text{-mhp})_2(PMe_3)_2$ was obtained by reacting $Mo_2(mhp)_4$ with $(CH_3)_3SiCl$ and PMe_3 in THF, as described for the synthesis of *cis*-$Mo_2Cl_2(6\text{-mhp})_2(PEt_3)_2$.[8] The resulting dark red product was chromatographed twice on silica gel with CH_2Cl_2 as an eluant. The ^1H NMR spectrum of the product is consistent with the proposed stoichiometry, and the presence of only a singlet at −6.99 ppm in the $^{31}P\{^1H\}$ NMR spectrum is consistent with the results obtained for the complex with PR_3 = PEt_3.[9] The literature procedure describing the preparation of $Mo_2Cl(6\text{-mhp})_3(PMePh_2)$[9] was modified by refluxing *cis*-$Mo_2Cl_2(6\text{-mhp})_2(PMe_2Ph)_2$ and 1 equiv of Hmhp in toluene to afford $Mo_2Cl(6\text{-mhp})_3(PMe_2Ph)$.

Instrumentation and Procedures. Electronic absorption spectra were recorded on an OLIS-modified Cary 17D or Cary 2300 UV−vis−near-IR spectrometer. Extinction coefficients were calculated from Beer−Lambert plots composed of at least seven points. The emission spectra were obtained by exciting samples at 546.5 nm with the 200 W Hg/Xe lamp of a spectrometer designed and constructed at Michigan State University.[12] Temperature-dependent emission spectra were obtained by controlling the temperature of microcrystalline solids with an Air Products cryogenic system. Emission quantum yields were measured using $Ru(bpy)_3Cl_2$ in H_2O as a quantum yield standard (Φ_e = 0.042[13]). Both ^{31}P and ^1H NMR spectra were recorded on a Varian VXR-300S spectrometer at 121 and 300 MHz, respectively. ^1H NMR spectra were referenced to the residual protons of incompletely deuterated solvents and $^{31}P\{^1H\}$NMR spectra were referenced to an external sample of 85% aqueous H_3PO_4. Luminescence lifetime measurements were made utilizing a previously described time-correlated single-photon-counting instrument,[14] housed in the LASER Laboratory at Michigan State. Fluorescence decays were obtained with exciting and detecting wavelengths of 580 and 640 nm, respectively. Sample irradiations were performed using an Oriel 1000 W Hg/Xe high-pressure lamp. The beam was collimated and passed through a circulating water bath, and excitation wavelengths were selected with Schott high-energy cutoff filters. Photolysis experiments were performed in two-arm evacuable cells equipped with Kontes quick-release Teflon valves. Sample temperatures were held at 10.0 ± 0.5 °C for all photochemical experiments. Photochemical quantum yields were determined using an identical setup, except that the reaction temperature was 15 ± 0.5 °C and Oriel interference filters were used in place of the cutoff filters. The intensity of the lamp was determined using a ferrioxalate actinometer.[15] Photoproduct concentrations were limited to less than 10% to avoid inner filter effects and competing product absorption. The quantum yields were determined by monitoring the disappearance of the $\delta \rightarrow \delta^*$ absorption band of the starting complex. The overall chemical yields for the photoreaction were determined from electronic absorption spectra of the photolyzed solutions by simultaneously solving Beer's law at three wavelengths.

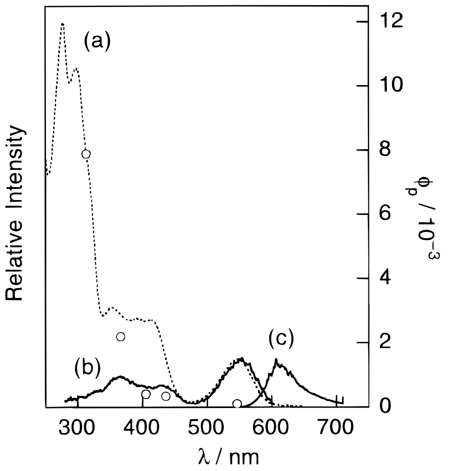

Figure 1. (a) Absorption, (b) fluorescence excitation, and (c) emission spectra of *cis*-$Mo_2Cl_2(6\text{-mhp})_2(PMe_2Ph)_2$ in deoxygenated 2-methylpentane at room temperature. The absorption and excitation spectra are normalized to each other on the basis of the intensity of the $\delta \rightarrow \delta^*$ transition. The open circles are the quantum yields for the photoreaction of *cis*-$Mo_2Cl_2(6\text{-mhp})_2(PMe_2Ph)_2$ in benzene at the specified wavelengths.

Results

Dichloromethane solutions of *cis*-$Mo_2Cl_2(6\text{-mhp})_2(PR_3)_2$ exhibit characteristic $M\overset{4}{-}M$ absorption profiles dominated by a lowest energy absorption in the ~550 nm spectral range. With the exception of that of the PMe_3 complex, the absorption spectra of *cis*-$Mo_2Cl_2(6\text{-mhp})_2(PR_3)_2$ complexes have previously been investigated.[8,9] The prominent low-energy feature is consistent with a $\delta \rightarrow \delta^*$ transition. Deconvolution of the electronic absorption spectrum of the PEt_3 complex suggests the presence of at least five other bands,[8] and tentative assignments for some of these have been made by comparison to the assigned spectra of $Mo_2(mhp)_4$ and $Mo_2Cl_4(PR_3)_4$. Important to the studies reported here, the intense absorptions at 300 and 280 nm have been assigned[8] to ligand-to-metal charge transfer (LMCT) and mhp-localized $\pi \rightarrow \pi^*$ transitions.

Figure 1 shows the absorption, fluorescence excitation, and emission spectra for the PMe_2Ph complex. Excitation into the $\delta \rightarrow \delta^*$ transition of room temperature solutions and solids of the complexes produces bright luminescence that is easily

---

(8) Fanwick, P. E. *Inorg. Chem.* **1985**, *24*, 258−63.
(9) Harwood, W. S.; Kennedy, S. M.; Lytle, F. E.; Qi, J.; Walton, R. A. *Inorg. Chem.* **1987**, *26*, 1784−8.
(10) Trogler, W. C.; Gray, H. B. *Acc. Chem. Res.* **1978**, *11*, 232−9.
(11) Bursten, B. E.; Kaufmann, G. B. *Inorg. Chem.* **1985**, *24*, 1165−9.
(12) Mussell, R. D.; Nocera, D. G. *J. Am. Chem. Soc.* **1988**, *110*, 2764−72.
(13) Van Houten, T.; Watts, R. J. *J. Am. Chem. Soc.* **1976**, *98*, 4853−8.
(14) Bowman, L. E.; Berglund, K. A.; Nocera, D. G. *Rev. Sci. Instrum.* **1993**, *64*, 338−41.
(15) Ferraudi, G. J. *Elements of Inorganic Photochemistry*; Wiley: New York, 1988; Chapter 1.5.

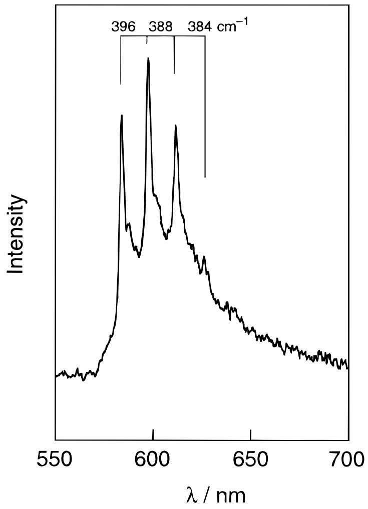

Figure 2. Corrected emission spectrum of a solid sample of *cis*-$Mo_2Cl_2(6\text{-}mhp)_2(PEt_3)_2$ at 10 K.

Table 1. Photophysical Data for *cis*-$Mo_2Cl_2(6\text{-}mhp)_2(PR_3)_2$ Complexes in CH_2Cl_2 at Room Temperature

R_3	$\lambda_{\text{max,abs}}(\delta\rightarrow\delta^*)$/nm	$\lambda_{\text{max,em}}(\delta^*\rightarrow\delta)$/nm	Φ_{em}	τ/ns
Me_3	545	600	0.084	50
Et_3	542	605	0.22	75
Me_2Ph	545	607	0.11	45
$MePh_2$	549	614	0.18	74

observed, even in ambient light. As the wavelength of excitation is decreased, the overall emission emanating from the complex is severely attenuated. This is most easily observed by comparing the excitation and absorption spectra. Using the $\delta \rightarrow \delta^*$ transition to standardize intensities, the intensity of the excitation profile is attenuated significantly in the 325−425 nm spectral region and disappears completely when the excitation wavelength is coincident with the near-UV charge transfer transitions (λ <325 nm).

Upon cooling to 10 K, the emission of the PMe_2Ph and PEt_3 complexes blue-shifts and sharpens with the fwhm of the emission band changing from ~1500 to ~990 cm^{-1}. These data suggest that the emission profile is inhomogeneously broadened owing to luminescence from different conformers of the complex. With cooling, the conformer contributing the higher energy luminescence to the overall emission profile is preferred. Interestingly, the temperature dependence of the emission profile of the $PMePh_2$ complex is nearly negligible, suggesting the presence of a dominant conformer at all temperatures. The Stokes shifts between the absorption and emission profiles of room-temperature solution spectra are modest, ranging from 1850 cm^{-1} for $PR_3 = PMe_3$ to 2010 cm^{-1} for $PR_3 = PMe_2Ph$, and smaller than those observed for the $Mo_2Cl_4(PR_3)_4$ series (2210 cm^{-1} for $PR_3 = PMe_3$,[16] 2210 cm^{-1} for $PR_3 = PBu_3$,[17] and 2250 cm^{-1} for $PR_3 = PEt_3$[18]). This result suggests less distortion in *cis*-$Mo_2Cl_2(6\text{-}mhp)_2(PR_3)_2$ excited states owing to more hindered elongation of the metal−metal bond when it is spanned by the rigid, bidentate mhp ligands as compared to the $Mo_2Cl_4(PR_3)_4$ series where the metal−metal bond is unsupported by bridging ligands.

Luminescence spectra feature sharp vibrational fine structure when solid samples of *cis*-$Mo_2Cl_2(mhp)_2(PR_3)_2$ are cooled to $T < 50$ K. The emission spectrum for *cis*-$Mo_2Cl_2(6\text{-}mhp)_2(PEt_3)_2$ at 10 K (Figure 2) is representative of the data obtained for the *cis*-$Mo_2Cl_2(6\text{-}mhp)_2(PR_3)_2$ series of compounds. The $\delta \rightarrow \delta^*$ absorption band is a mirror image of the emission band and the 0−0 components of the two profiles overlap, indicating the absence of a Duschinsky effect.[19] These results are consistent with emission originating from the $\delta\delta^*$ excited state in which distortion occurs along a coordinate common to both excited and ground states; the prominent vibrational progression is a signature of distortion along the metal−metal bond. The frequency of the progression for *cis*-$Mo_2Cl_2(6\text{-}mhp)_2(PR_3)_2$ (389 ± 4, 387 ± 4, and 383 ± 15 cm^{-1} for $PR_3 = PEt_3$, PMe_2Ph and $PMePh_2$, respectively) reasonably lies between the 358 and 425 cm^{-1} frequencies of the ν_{a_1}(Mo−Mo) symmetric stretches of $Mo_2Cl_4(PMe_3)_4$ and $Mo_2(mhp)_4$, respectively.[16,20] Low-temperature absorption spectra of the $\delta \rightarrow \delta^*$ transition of the PEt_3 complex place $\nu_{a_1'}$(Mo−Mo) at 370 cm^{-1}. A 19 cm^{-1} reduction of the metal−metal frequency in the $\delta\delta^*$ excited state of *cis*-$Mo_2Cl_2(6\text{-}mhp)_2(PEt_3)_2$ is in good agreement with the 22 cm^{-1} decrease of ν_{a_1}(Mo−Mo) in electronically excited $Mo_2Cl_4(PMe_3)_4$ and is within the 10−50 cm^{-1} range typically observed for $M\overset{4}{—}M$ complexes.[21] The Mo−Mo bond distances in the ground and excited states can be calculated from the vibronic progressions of the low-temperature emission and absorption spectra, respectively, by using Woodruff's modification of Badger's relation.[22] The 389 cm^{-1} progression in the emission spectrum of the PEt_3 complex corresponds to a ground state Mo−Mo bond distance of 2.10 Å, which is in excellent agreement with the 2.103 Å distance obtained from the crystal structure.[8] Moreover a 0.048 Å increase of the Mo−Mo bond distance in the excited state, as determined from the 370 cm^{-1} progression in the low-temperature absorption spectrum, results from the elimination of the weak δ bond upon $\delta \rightarrow \delta^*$ excitation. This elongation coincides with the ~0.025−0.050 Å increase in M−M bond length when the δ bond is eliminated by chemical redox.[23,24]

The luminescence quantum yields (Φ_e) of *cis*-$Mo_2Cl_2(6\text{-}mhp)_2(PR_3)_2$ in CH_2Cl_2 are listed in Table 1. Generally they are greater than those observed for the corresponding $Mo_2Cl_4(PR_3)_4$ complexes. Similarly, the lifetimes of *cis*-$Mo_2Cl_2(6\text{-}mhp)_2(PR_3)_2$ complexes are also longer than those of their $Mo_2Cl_4(PR_3)_4$ congeners. Although solutions of the complexes exhibit clean monoexponential luminescence decays, the lifetimes of solid samples at room temperature and at 77 K show a second component. In view of the monoexponential behavior of these solids when dissolved in solution, the second component does not appear to arise from an impurity but is a consequence of localized heating of the lattice or some other crystal lattice effect. In addition to CH_2Cl_2, luminescence lifetimes and emission quantum yields, listed in Table 2, were measured in the solvents in which photochemical studies were performed. These data reveal no discernible trend with respect to solvent properties.

The irradiation of solutions of *cis*-$Mo_2Cl_2(6\text{-}mhp)_2(PR_3)_2$ complexes with visible and near-UV light results in a prompt reaction. In the absence of light, no reaction is observed, though

---

(16) Hopkins, M. D.; Gray, H. B. *J. Am. Chem. Soc.* **1984**, *106*, 2468−9.

(17) Miskowski, V. M.; Goldbeck, R. A.; Kliger, D. S.; Gray, H. B. *Inorg. Chem.* **1979**, *18*, 86−9.

(18) Zietlow, T. C.; Hopkins, M. D.; Gray, H. B. *J. Solid State Chem.* **1985**, *57*, 112−9.

(19) Ballhausen, C. J. *Molecular Electronic Structures of Transition Metal Complexes*; McGraw-Hill: New York, 1979; Chapter 1.

(20) Manning, M. C.; Trogler, W. C. *J. Am. Chem. Soc.* **1983**, *105*, 5311−20.

(21) Cotton, F. A.; Walton, R. A. *Multiple Bonds Between Metal Atoms*, 2nd ed.; Oxford: New York, 1993; p 739.

(22) Miskowski, V. M.; Dallinger, R. F.; Christopher, G. C.; Morris, D. E.; Spies, G. H.; Woodruff, W. H. *Inorg. Chem.* **1987**, *26*, 2127−32.

(23) Reference 21, p 633.

(24) Hsu, T.-L. C.; Chang, I.-J.; Ward, D. L.; Nocera, D. G. *Inorg. Chem.* **1994**, *33*, 2932−7.

Table 2. Solvent Dependence of Selected Photophysical Data and Photolysis Quantum Yields for *cis*-$Mo_2Cl_2(6\text{-mhp})_2(PMe_2Ph)_2$

solvent	Φ_{em}	τ/ns	$\Phi_p{}^a$
DMF	0.084	50	0.084
THF	0.22	75	0.22
C_6H_6	0.18	74	0.18

[a] Photolysis quantum yield for the disappearance of *cis*-$Mo_2Cl_2(6\text{-mhp})_2(PMe_2Ph)_2$ with 405-nm irradiation.

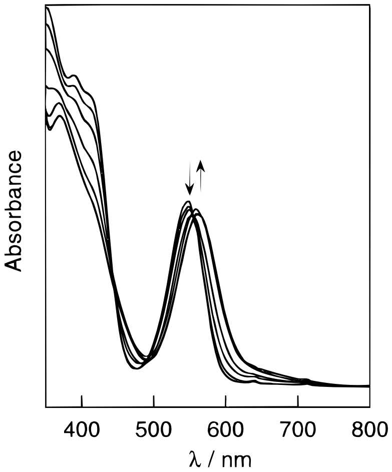

Figure 3. Electronic absorption spectral changes during the photolysis (λ_{exc} >435 nm) of *cis*-$Mo_2Cl_2(6\text{-mhp})_2(PMe_2Ph)_2$ in deoxygenated benzene at 10 °C. Spectra were recorded at 0, 10, 30, 70, 170, 300, and 390 min.

a thermal reaction for DMF solutions occurs at elevated temperatures (>60 °C). Because all members of this series photoreact in a similar manner, we focus on the photochemistry of only one of these complexes, *cis*-$Mo_2Cl_2(6\text{-mhp})_2(PMe_2Ph)_2$.

Irradiation of the benzene solutions of *cis*-$Mo_2Cl_2(6\text{-mhp})_2(PMe_2Ph)_2$ with visible light (λ >435 nm) causes the bright red solution to turn plum. The spectral changes associated with this photochemistry are displayed in Figure 3. The disappearance of the $\delta \rightarrow \delta^*$ absorption at 548 nm is accompanied by the appearance of an absorption band at slightly longer wavelengths. Photolyzed solutions eluted on silica gel with CH_2Cl_2 yield major components that are red and purple, and minor components that are blue and orange.

All the components observed by column chromatography have been identified. The red component is unreacted starting material, identified on the basis of its $^{31}P\{^1H\}$NMR and electronic absorption spectra. The UV−vis spectrum of the purple product exhibits maxima at 573 and 329 nm, with shoulders observed at 417 and 367 nm. The $^{31}P\{^1H\}$NMR spectrum of the purple component exhibits two resonances, a doublet at 1.35 ppm and a triplet at 0.88 ppm (J(P−P) = 12.8 Hz; doublet:triplet ratio is 2:1). These UV−vis and $^{31}P\{^1H\}$NMR spectra identically match the corresponding spectra of the independently prepared compound $Mo_2Cl_3(6\text{-mhp})(PMe_2Ph)_3$.[9] This compound was first observed as an impurity in the synthesis of $Mo_2Cl_2(6\text{-mhp})_2(PMe_2Ph)_2$ and can be directly synthesized by reacting *cis*-$Mo_2Cl_2(6\text{-mhp})_2(PMe_2Ph)_2$ with $Mo_2Cl_4(PMe_2Ph)_4$ in refluxing toluene. The blue, minor product is also readily identified from its spectroscopic signatures; the electronic absorption and NMR spectral features are identical to those of $Mo_2Cl_4(PMe_2Ph)_4$. The orange product was present in smaller amounts and decomposed before eluting from the column. Nevertheless we were able to identify the complex as $Mo_2Cl(6\text{-mhp})_3(PMe_2Ph)$ on the basis of TLC by using an independently prepared sample as a standard.

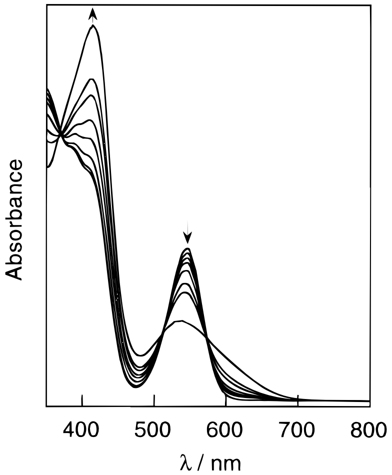

Figure 4. Electronic absorption spectral changes during the photolysis (λ_{exc} >435 nm) of *cis*-$Mo_2Cl_2(6\text{-mhp})_2(PMe_2Ph)_2$ in deoxygenated DMF at 10 °C. Spectra were recorded at 0, 15, 45, 90, 180, 315, 435, and 1110 min.

The disappearance quantum yield of the photolysis reaction of *cis*-$Mo_2Cl_2(6\text{-mhp})_2(PMe_2Ph)_2$ in benzene was measured at several wavelengths; these are shown overlayed on the absorption spectrum of Figure 1. The quantum yield changes only slightly over the excitation wavelength range from 546 to 405 nm and increases dramatically for λ_{exc} < 366 nm. In the presence of a 20-fold excess of Hmhp, the quantum yield decreases from 2.2×10^{-3} to 4.7×10^{-4} at λ = 366 nm. Interestingly, the photoreaction is accelerated by Cl^- (the quantum yield increased by almost a factor of 10). Similar photoreaction quantum yields are observed for the other complexes in this series. For instance, $\Phi_p{}^{366} = 7.8 \times 10^{-4}$ for *cis*-$Mo_2Cl_2(6\text{-mhp})_2(PEt_3)_2$ in benzene. Photochemical substitution of mhp in benzene is also observed for *cis*-$Mo_2Cl_2(6\text{-mhp})_2(PMePh_2)_2$. However, its low solubility precludes an accurate quantum yield determination.

The photolysis reaction of *cis*-$Mo_2Cl_2(6\text{-mhp})_2(PMe_2Ph)_2$ is strongly solvent dependent. As opposed to the plum-colored benzene-photolyzed solutions, irradiation in DMF (λ_{exc} >435 nm) leads to bright orange solutions, the spectral changes for which are displayed in Figure 4. The reaction is complete within a day and the absorption spectrum of the photoproduct compares well with that of *cis*-$Mo_2Cl(6\text{-mhp})_3(PMe_2Ph)$. If the irradiation is continued for several more hours, the peak at 528 nm shifts to 514 nm and the 417-nm band grows in intensity but is energetically invariant. This secondary photoreaction is identical to the one that occurs when independently synthesized $Mo_2Cl(6\text{-mhp})_3(PMe_2Ph)$ is irradiated (λ >435 nm) in DMF.

The photochemistry of *cis*-$Mo_2Cl_2(6\text{-mhp})_2(PMe_2Ph)_2$ in THF is straightforward. Photolysis yields a blue-gray solution, and as Figure 5 shows, the low-energy tail of the $\delta \rightarrow \delta^*$ absorption increases in intensity and a broad prominent absorption appears at 403 nm. An isosbestic point is maintained at low energy; however, the absence of an isosbestic point in the near-ultraviolet spectral region indicates the presence of a minor impurity. The two major photoproducts were separated by column chromatography as described above. The purple and red-orange photoproducts, $Mo_2Cl_3(6\text{-mhp})(PMe_2Ph)_3$ and $Mo_2Cl(6\text{-mhp})_3(PMe_2Ph)$, were isolated in nearly equal yields in addition to unreacted starting material.

The photoproducts exhibit different stabilities in the various solvents used to carry out the photochemistry. In THF, both the $Mo_2Cl_3(6\text{-mhp})(PMe_2Ph)_3$ and $Mo_2Cl(6\text{-mhp})_3(PMe_2Ph)$ photoproducts are stable. When solutions are allowed to stand at room temperature, protected from light, the absorption

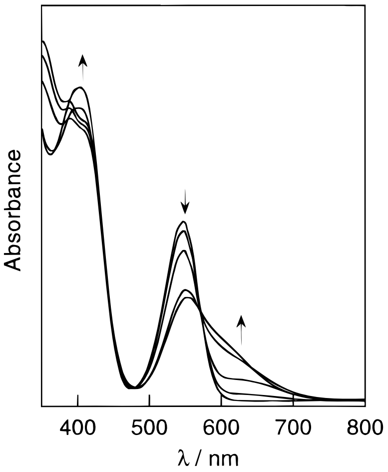

Figure 5. Electronic absorption spectral changes during the photolysis (λ_{exc} >435 nm) of *cis*-$Mo_2Cl_2(6\text{-mhp})_2(PMe_2Ph)_2$ in deoxygenated THF at 10 °C. Spectra were recorded at 0, 10, 30, 120, and 180 min.

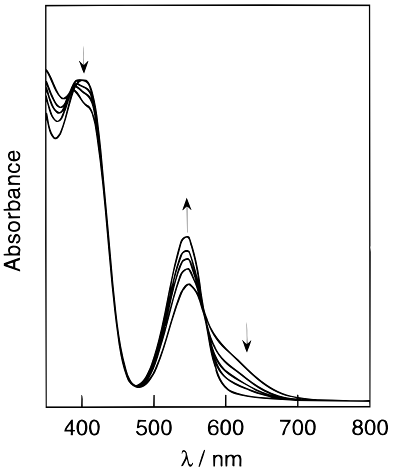

Figure 6. Electronic absorption spectral changes recorded 30, 110, 210, 340, and 1260 min after the conclusion of the photolysis shown in Figure 5. The sample was stored in the dark at room temperature.

spectrum of the starting complex reappears over hours. As indicated by electronic absorption spectra in Figure 6, this back-reaction to give *cis*-$Mo_2Cl_2(6\text{-mhp})_2(PMe_2Ph)_2$ appears to be clean and is reproduced by mixing equimolar amounts of $Mo_2Cl_3(6\text{-mhp})(PMe_2Ph)_3$ and $Mo_2Cl(6\text{-mhp})_3(PMe_2Ph)$ in the presence of free ligand. The reaction is accelerated when the conjugate base of the ligand is generated by the addition of 1,8-bis(dimethylamino)naphthalene to solution. Similarly, the reaction is accelerated when the tetrabutylammonium salt of the mhp anion is added to solution. No thermal reaction is observed in the absence of ligand or its conjugate base. In benzene, the back-reaction only partially occurs because $Mo_2Cl(6\text{-mhp})_3(PMe_2Ph)$ is depleted by a competing, albeit slow, secondary photochemical reaction. A secondary photoreaction of $Mo_2Cl(6\text{-mhp})_3(PMe_2Ph)$ was verified by photolyzing benzene solutions of the independently prepared complex. Conversely in DMF, whereas $Mo_2Cl(6\text{-mhp})_3(PMe_2Ph)$ is stable, $Mo_2Cl_3(6\text{-mhp})(PMe_2Ph)_3$ is not. DMF solutions of $Mo_2Cl_3(6\text{-mhp})(PMe_2Ph)_3$ undergo slow thermal and rapid photochemical decomposition, thereby explaining the complete absence of a thermal back-reaction for DMF-photolyzed solutions.

Discussion

The photochemistry of *cis*-$Mo_2Cl_2(6\text{-mhp})_2(PR_3)_2$ complexes in homogeneous solution is ligand redistribution to give $Mo_2Cl_3(6\text{-mhp})(PR_3)_3$ and $Mo_2Cl(6\text{-mhp})_3(PR_3)$ as major photoproducts. Depending on the solvent, the overall photochemistry of the system varies owing to different stabilities of the mono- and trisubstituted mhp species. Scheme 2 summarizes the overall photoreactivity. The mono- and trisubstituted photoproducts are stable in THF solutions, and they back-react in the dark over hours to produce the red parent complex of *cis*-$Mo_2Cl_2(6\text{-mhp})_2(PR_3)_2$. The overall chemical yield for each of the photoproducts in THF is 45(±10)%. This is not the case in DMF solutions, where the monosubstituted mhp product is thermally and photochemically unstable. The facile decomposition of the monosubstituted complex circumvents its reaction with the trisubstituted complex to regenerate starting complex. Thus only the orange solution of $Mo_2Cl(6\text{-mhp})_3(PR_3)$ is obtained for photolysis reactions performed in DMF. Conversely, in benzene, the trisubstituted product undergoes a secondary photoreaction and only the purple solution of $Mo_2Cl_3(6\text{-mhp})(PR_3)_3$ is obtained. Because the ensuing photoreaction of $Mo_2Cl(6\text{-mhp})_3(PR_3)$ is slow, a partial back-reaction to *cis*-$Mo_2Cl_2(6\text{-mhp})_2(PR_3)_2$ is observed over days. The determination of chemical yields from the photolysis spectra of DMF and benzene solutions are compromised by the presence of absorption contributions from the decomposition products.

The wavelength dependence of the quantum yield shows that the reaction is efficiently promoted by λ_{exc} <366 nm. Specifically, Φ_p appears to track the absorption profile of the 300 nm absorption band, which is in the region for $\sigma_{MP} \rightarrow \delta^*$ LMCT transitions of molybdenum−halide $M\overset{4}{-}M$ complexes.[25] The photochemistry is appreciably maintained at 366 nm because the excitation wavelength clearly lies within the low-energy tail of this intense near-UV transition. Photoreactivity from the LMCT excited state is also consistent with the excitation spectrum of *cis*-$Mo_2Cl_2(6\text{-mhp})_2(PMe_2Ph)_2$ in hydrocarbon solvent. The intensity of the excitation profile is attenuated in the 325−400 nm range and is negligible at wavelengths coincident with the $\sigma_{MP} \rightarrow \delta^*$ LMCT transition.[26] This type of behavior implies that a unimolecular photoreaction is a significant process for the high-energy excited states of these complexes. It is noteworthy that the fluorescence excitation and absorption spectra are identical for excitation wavelengths as short as 220 nm for hydrocarbon solutions of $Mo_2X_4L_4$ compounds, which are photoinert under these conditions.[27] The photochemistry reported here is consistent with a LMCT parentage to the extent that a $\sigma_{MP} \rightarrow \delta^*$ excitation would lead to a weakening of the metal−ligand bonds as the formal oxidation state of the metal is reduced. The photoreaction quantum yield decreases significantly as the excitation wavelength is moved into the visible spectral region. A low photoreaction quantum yield is observed for wavelengths coincident with the $\delta \rightarrow \delta^*$ transition. Presumably, the photoreaction proceeds inefficiently with excitation of the metal-localized excited states.

The loss of mhp from the metal core is reflected in the solvent dependence of the photolysis quantum yields. Dissociation of mhp leads to ionic intermediates that will be stabilized by increasingly polar solvents. This is borne out by the monotonic increase of Φ_p at a given wavelength along the series C_6H_6 < THF < DMF (see Table 2). Interestingly, the emission quantum

---

[25] Hopkins, M. D.; Miskowski, V. M.; Gray, H. B. *J. Am. Chem. Soc.* **1988**, *110*, 1787−93.

[26] The higher transition centered at 280 nm is consistent with a mhp-localized $\pi \rightarrow \pi^*$ transition for *cis*-$Mo_2Cl_2(6\text{-mhp})_2(PR_3)_2$, as it is energetically coincident with this transition in the $Mo_2(mhp)_4$ complex.[20] Our photochemical studies did not include this spectral region.

[27] Miskowski, V. M.; Gray, H. B.; Hopkins, M. D. *Inorg. Chem.* **1992**, *31*, 2885−91.

Scheme 2

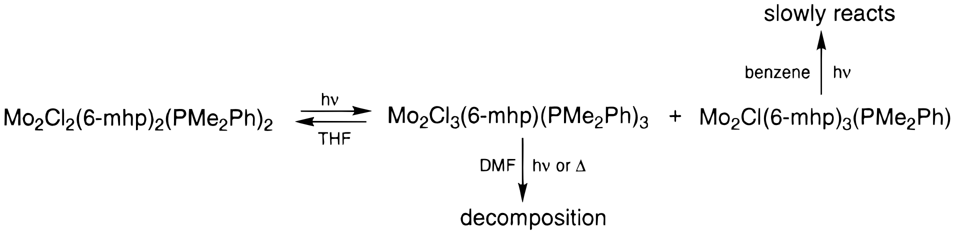

yields and lifetimes do not show a parallel trend. Inasmuch as photodissociation of a mhp ligand is a single contributing factor to the overall nonradiative decay pathway for *cis*-$Mo_2Cl_2(6\text{-mhp})_2(PR_3)_2$ complexes, the inability to correlate Φ_p with Φ_e (or τ_0) indicates that the overall nonradiative decay is influenced by other factors in addition to ligand dissociation from the excited state. Moreover, mhp loss may be more complicated than direct excited state dissociation, as evidenced by the Cl^- enhancement of the observed photoreactivity. A primary photoprocess involving Cl^- dissociation could in principle catalyze the dissociation of the mhp ligand.

The results described here suggest that any potential photochemistry of these complexes to new products such as Mo^{III}_2 W-frame complexes will be circumvented by photosubstitution of the bidentate mhp ligands. This obstacle might be overcome by the substitution of the mhp ligands with tetradentate ligands that enforce the same cis conformation. Recently, the $M\overset{4}{—}M$ Schiff base complex $Mo_2(N_4)(O_2CCH_3)_2$ has been synthesized where N_4 is 5,7,12,14-tetramethyldibenzo[*b*,*i*][1,4,8,11]tetraazocyclotetradecine.[28] By using existing synthetic methodologies,[29] it may be possible to replace the acetates with the appropriate ligands to give *cis*-$Mo_2(NN)Cl_2(PR_3)_2$. We are currently investigating the design of such systems with the goal of elucidating the photophysics and photochemistry of such complexes.

Acknowledgment. We thank Jeffrey Zaleski and James Roberts for assistance with lifetime measurements. Financial support of this work by National Science Foundation Grant CHE-9521347 is gratefully acknowledged.

IC960252U

---

(28) Kerbaol, J. M.; Furet, E.; Guerchais, J. E.; LeMest, Y.; Saillard, J. Y.; Sala-Pala, J.; Toupet, L. *Inorg. Chem.* **1993**, *32*, 713−21.

(29) Green, M. L. H.; Parkin, G.; Bashkin, J.; Fail, J.; Prout K. *J. Chem. Soc., Dalton Trans.* **1982**, 2519−25.